

Soils Reveal Widespread Manganese Enrichment from Industrial Inputs

ELIZABETH M. HERNDON,^{*,†,‡}
LIXIN JIN,^{†,‡} AND SUSAN L. BRANTLEY^{†,‡}
*Department of Geosciences, The Pennsylvania State University,
University Park, Pennsylvania 16802, United States,
and Center for Environmental Kinetics Analysis, Earth and
Environmental Systems Institute, The Pennsylvania State
University, University Park, Pennsylvania 16802, United States*

Received June 13, 2010. Revised manuscript received
November 16, 2010. Accepted November 18, 2010.

It is well-known that metals are emitted to the air by human activities and subsequently deposited to the land surface; however, we have not adequately evaluated the geographic extent and ecosystem impacts of industrial metal loading to soils. Here, we demonstrate that atmospheric inputs have widely contaminated soils with Mn in industrialized regions. Soils record elemental fluxes impacting the Earth's surface and can be analyzed to quantify inputs and outputs during pedogenesis. We use a mass balance model to interpret details of Mn enrichment by examining soil, bedrock, precipitation, and porefluid chemistry in a first-order watershed in central Pennsylvania, USA. This reveals that ~53% of Mn in ridge soils can be attributed to atmospheric deposition from anthropogenic sources. An analysis of published data sets indicates that over half of the soils surveyed in Pennsylvania (70%), North America (60%), and Europe (51%) are similarly enriched in Mn. We conclude that soil Mn enrichment due to industrial inputs is extensive, yet patchy in distribution due to source location, heterogeneity of lithology, vegetation, and other attributes of the land surface. These results indicate that atmospheric transport must be considered a potentially critical component of the global Mn cycle during the Anthropocene.

Introduction

Manganese (Mn), the 12th most abundant element in the Earth's crust, is predominantly found in soils as fine-grained, poorly crystalline oxides (1, 2). A small fraction of global Mn is present in the atmosphere. This Mn has been attributed to both anthropogenic emissions and wind erosion of soils; however, Mn pollution may overshadow mineral dust in industrialized regions and can disseminate widely as dust particulates or solutes in rain (3–13). Steel and ferroalloy manufacturing have historically been the primary sources of anthropogenic Mn emissions (3); however, Mn has also been used as an additive in gasoline, and coal combustion has recently become a dominant industrial source of atmospheric Mn (3, 11).

Most Mn-compounds in soils comprise highly reactive constituents that influence the mobility of heavy metals (Co,

Ni, Cu, Zn, Mo) and participate in abiotic and microbial redox reactions that can affect soil fertility (14). For example, high Mn bioavailability in soils has led to tree toxicity and forest decline in the northeastern United States (15, 16). Additionally, Mn is regulated as a human health hazard by the United States Environmental Protection Agency (EPA) due to well-established links between respirable Mn and neurological disorders (3, 12).

Although Mn levels in the air have declined since monitoring began (3, 5), there are no data available prior to the 1950s that can be used to assess total deposition over industrial time scales. However, past deposition of atmospheric Mn can be deciphered from soil profiles. These depth profiles record inputs, outputs, and internal redistribution processes and can be used to quantify influences on soil development, including past inputs from the air (17–21). For example, soil profiles that exhibit net enrichment of certain elements relative to parent material are interpreted as addition profiles, while other profiles that document net depletion due to natural weathering processes are interpreted as depletion profiles (22).

Integrated soil, geologic, ecologic, and hydrologic observations are necessary to decipher long-term records of chemical processes in the soil. Such observations are now available for the Susquehanna Shale Hills Observatory (SSHO; Figure S1), one of six Critical Zone Observatories (CZO) in the United States and the focus of multidisciplinary characterization (23–26). The Critical Zone is defined as the region of the Earth's surface extending from groundwater to the top of vegetation that includes complex interactions among water, air, rock, soil, and biota (27). Our detailed soil characterization at SSHO reveals that Mn is commonly observed as an addition profile, while the geochemically similar element Fe is consistently present as a depletion profile. Like iron, manganese is mobilized under acidic soil conditions such as those present at Shale Hills; however, Mn-oxide solubilization occurs at higher pH values than is observed for Fe, potentially leading to greater Mn losses (28). The concurrent Fe depletion and Mn enrichment observed at SSHO can be explained by loss of Fe to weathering but gain of Mn due to atmospheric inputs.

We hypothesized that atmospheric contamination from industrial activity caused the observed Mn enrichment in SSHO soils. The SSHO is located in Huntingdon County, Pennsylvania, USA, an epicenter for iron production in the early 19th century that contained approximately 87 operational furnaces and forges at its peak in 1840. Forty-seven of these furnaces, including Monroe Furnace (4 km from SSHO), were located in Huntingdon County (29). In this study, we quantify excess soil Mn at SSHO and develop a mass balance model to estimate rates of atmospheric input over industrial and geologic time scales. Additionally, we analyze soils near a modern steel factory in Burnham, PA to demonstrate Mn enrichment near a point source. Our observations of local Mn enrichment led us to analyze databases of Pennsylvania, U.S., and European soils in order to ascertain broader geographic patterns of Mn enrichment in soils. These databases, along with our specific observations for SSHO and Burnham soils, lead to the conclusion that the topsoils of industrialized regions are widely contaminated with patchy occurrences of excess Mn.

Methods

Sampling Locations. SSHO is a 7.9-ha first-order catchment located within the Juniata watershed and larger Susquehanna river basin. SSHO contains residual and colluvial soils derived

* Corresponding author phone: (814)865-8055; e-mail eherndon@psu.edu.

[†] Department of Geosciences.

[‡] Center for Environmental Kinetics Analysis, Earth and Environmental Systems Institute.

from the Silurian-aged Rose Hill shale formation, an oxidized, organic-poor shale that extends throughout the Appalachian region. Here, soils are thin, well-drained Inceptisols on the ridges (thicknesses <0.5 m) which transition downslope toward thicker Ultisols in the valley and swales (<3 m) (23, 24). Annual precipitation in the Shale Hills region is $\sim 105 \text{ cm y}^{-1}$, and rainwater is currently acidic (average pH 4.35) and enriched in nitrate and sulfate (30). The vegetation is dominated by oak species with smaller populations of hickory, maple, hemlock, and pines.

Soil cores were excavated with a stainless steel auger to point of refusal, the depth to which we could manually auger and our closest approximation for the soil-bedrock interface (25), at 21 locations along the SSHO ridge. Each core was sampled in 2–12 cm depth intervals starting at the top of mineral soil and ending at the soil-bedrock interface. Given this sampling methodology, our definition here for “soil” is all material that could be sampled with a hand auger and had an average thickness (L) of 32 cm.

Pore water samples were collected between 2006–2009 from four tension lysimeters installed at the soil-bedrock interface (30–40 cm depth) at two ridgetop locations on the north and south slopes. Samples were collected approximately biweekly during wet periods when sufficient soil moisture was available. The porous ceramic cups of the lysimeters have a maximum pore size of $1.3 \mu\text{m}$, so pore water samples were not further filtered after collection.

Representative precipitation samples ($n = 61$) collected in 2002 by the National Atmospheric Deposition Program (NADP) were obtained from sites PA-42 and PA-15 located 2.5 km and 14.5 km from SSHO. Precipitation samples were collected in plastic buckets, and we analyzed samples of the distilled water used to rinse the buckets to determine potential trace metal contamination.

Our second field location, Burnham, PA, is located approximately 28 km southeast of SSHO and has supported steel manufacturing since 1795. Burnham is bordered to the north by Jack’s Mountain, a Tuscarora sandstone ridge with soil-mantled slopes developed on the Silurian Clinton group (S_c) containing Rose Hill shale and Keefer sandstone, undifferentiated Bloomsburg claystone and Mifflintown shale (S_{bm}), and Wills Creek shale (S_{wc}) (31, 32). Twelve soil cores were augered to point of refusal at 10 locations between 1.1 and 23.8 km from the steel plant. The closest two sampling sites were located in Burnham on S_{wc} and S_{bm} . The other eight sampling sites were located along the slope of Jack’s Mountain on the Rose Hill and Wills Creek shales.

Chemical Analyses. To determine the total concentration of major elements (e.g., Mn, Ti, Zr) in soils, representative air-dried bulk samples that included all rock fragments, sand, silt, and clay particles at each depth were ground to pass a 100-mesh sieve (<149 μm), fused with lithium metaborate at 950 °C, and dissolved in 5% HNO_3 for analysis on a Leeman Laboratories PS3000UV inductively coupled plasma atomic emission spectrophotometer (ICP-AES) at the Penn State Materials Characterization Laboratory.

Pore water and precipitation samples were acidified with ultrapure concentrated HNO_3 and analyzed for cation concentrations on ICP-AES (pore water) or quadrupole ICP-mass spectrometry (precipitation). Anion concentrations in the water samples were measured using a Dionex ion chromatograph.

Results

SSHO Soils. For mineral soils sampled at SSHO ridges, the depth-weighted average Mn concentration ($C_{Mn,w} = 2200 \pm 2100 \mu\text{g g}^{-1}$; $n = 111$ samples) is elevated relative to the average concentration of the Rose Hill shale ($C_{Mn,p} = 800 \pm 300 \mu\text{g g}^{-1}$; $n = 24$ samples). This “parent rock” was drilled at the ridgetop and analyzed previously (25). The highest concen-

trations of Mn occur near the soil surface, with concentrations ranging up from 900 to 14,400 $\mu\text{g g}^{-1}$ in the uppermost soil sample from each core (Table S1).

SSHO Pore Waters and Precipitation. Pore fluids sampled at the soil-bedrock interface contain higher concentrations of Mn ($C_{Mn,pf} = 0.082 \pm 0.137 \mu\text{g mL}^{-1}$; $n = 66$) than influent precipitation ($C_{Mn,prt} = 0.0025 \pm 0.0024 \mu\text{g mL}^{-1}$; $n = 61$). Mn concentrations in the control samples of distilled water used to rinse the precipitation collectors showed no Mn contamination ($[\text{Mn}] < 0.00004 \mu\text{g mL}^{-1}$; $n = 7$). Chloride concentrations in the pore fluids ($C_{Cl,pf} = 1.35 \pm 1.02 \mu\text{g mL}^{-1}$; $n = 70$) are also high relative to influent precipitation as reported by the NADP (30) ($C_{Cl,prt} = 0.20 \pm 0.20 \mu\text{g mL}^{-1}$) and will be used to constrain the effects of evapotranspiration.

Burnham Soils. At Burnham, depth-averaged Mn concentrations in soils (340–1300 $\mu\text{g g}^{-1}$) are elevated relative to the deepest soil sampled from each core (100–600 $\mu\text{g g}^{-1}$) for 6 out of 7 soil cores augered within ~ 6 km of the Standard Steel facility (Table S2). In these cores, Mn concentrations are highest near the surface and decrease with depth. For the soil core augered closest to the facility (1.1 km), Mn concentrations are consistently high with depth (400–700 $\mu\text{g g}^{-1}$). Furthermore, the deepest sample remains high in Mn concentration (650 $\mu\text{g g}^{-1}$), and its Mn content may not be representative of parent material. In contrast, for soil cores sampled 6.6 to 15.8 km from the source, Mn concentrations are consistently low through the profiles (<400 $\mu\text{g g}^{-1}$). However, for the two soil cores augered ~ 24 km from the steel facility that lie within 50 m of a road, depth-averaged soil Mn concentrations are elevated (700 and 960 $\mu\text{g g}^{-1}$) relative to the deepest samples (310 and 390 $\mu\text{g g}^{-1}$).

Discussion

SSHO Soils. We use the mass transfer coefficient, $\tau_{i,j}$ to further investigate Mn concentrations in SSHO soils (eq 1). $\tau_{i,j}$ values indicate enrichment ($\tau_{i,j} > 0$) or depletion ($\tau_{i,j} < 0$) of a soluble element j in weathered material or soil (subscript w) relative to parent material (subscript p). The mass transfer coefficient accounts for variations in bulk density and concentration changes due to depletions or additions of other elements by ratioing concentrations of j to an insoluble element i such as Zr or Ti (17, 33)

$$\tau_{i,j} = \frac{C_{j,w}C_{i,p}}{C_{j,p}C_{i,w}} - 1 \quad (1)$$

Titanium (Ti) was measured in all samples and was observed to be relatively immobile. However, Zr shows less depletion than Ti in SSHO because its host mineral, zircon, is less soluble than Ti oxide (25). Depletion of Ti relative to Zr yielded average $\tau_{Zr,Ti} = -0.21$ in the 88 samples where Ti and Zr were both measured. Using $i = \text{Ti}$ may overestimate element addition and underestimate element depletion; therefore, Zr was used as the immobile element in eq 1. For the remaining 23 of 111 soil samples where Zr was not measured, Zr concentrations were estimated from measured Ti concentrations by using $\tau_{Zr,Ti} = -0.21$.

With Zr as the immobile element, all sampled ridge cores ($n = 21$) exhibit Mn in excess of parent material ($\tau_{Zr,Mn} > 0$). The enrichment, highest at the soil surface and decreasing to parent concentration at depth, is characteristic of an addition profile (22) (Figure 1). Specifically, mass balance requires that $\tau > 0$ documents external additions from natural sediments, direct anthropogenic inputs, or the atmosphere (22). In ridge soils such as those investigated here, sediment inputs are insignificant because the soils are situated at local topographic highs. Direct anthropogenic inputs are unlikely for SSHO given that the catchment has never been intensively farmed nor have the soils been moved or manipulated to

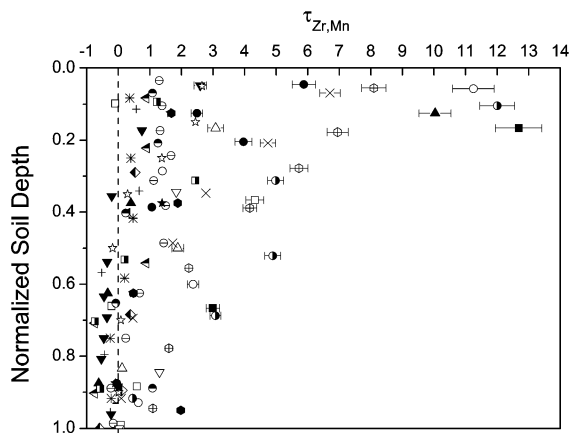


FIGURE 1. Normalized Mn concentrations ($\tau_{Zr,Mn}$, eq 1) are plotted as different symbols versus depth for 21 ridgetop soil cores at the Susquehanna Shale Hills Observatory (SSHO). Here, depth in the soil is normalized so that 1 = depth of the bedrock-soil interface. Soils document Mn enrichment ($\tau_{Zr,Mn} > 0$) near the surface that approaches underlying parent rock composition ($\tau_{Zr,Mn} = 0$) at depth. Surface soils are up to 13 times more enriched in Mn than parent. Error bars represent the propagated uncertainty in chemical analyses ($\pm 3\%$). Where no errors are shown, the bars are the size of symbols or smaller.

any great extent. Atmospheric inputs are left as the likely source of excess Mn.

Vegetation can recycle nutrients, enriching elements in the surface soil via litterfall while concurrently depleting the subsurface in that element through root uptake (34). However, vegetation alone cannot explain Mn enrichment of SSHO ridge top soils because there is insufficient Mn depletion in the subsurface. Therefore, the chemical data document net addition to the soil.

The mass of element j in soils per unit land surface area ($M_{j,w}$, mg cm^{-2}) can be estimated for one depth interval Δz (cm) as $M_{j,w} = \Sigma(\Delta z \cdot \rho_w \cdot C_{j,w})$. The total value for soil is calculated as a summation over all depths in the soil core (17). Here, ρ_w (g cm^{-3}) is the bulk density of the soil sample. Bulk density measurements previously obtained at SSHO were used to estimate bulk densities for each soil sample as a function of depth (Table S3). For this calculation, the sum of all sampling intervals must equal the total soil depth. $M_{Mn,w}$ averages $88.7 \pm 63.4 \text{ mg Mn cm}^{-2}$ in SSHO ridge soils (Table S1).

The *integrated mass outflux or influx*, $m_{j,w}$ (mg cm^{-2}), is the net loss ($m_{j,w} < 0$) or gain ($m_{j,w} > 0$) of j in the mineral soil relative to the Rose Hill shale parent (18). The shale bulk density (25) (ρ_p) has been measured at 2.42 g cm^{-3} . Values of $m_{j,w}$ are calculated by integration of $\tau_{i,j}$ over depth, z , from the mineral soil surface ($z = 0$) to the depth of auger refusal (L). This integration is corrected for volume strain (ϵ) following previous authors (17, 35)

$$m_{j,w} = C_{j,p} \rho_p \int_0^L \frac{\tau(z)}{\epsilon(z) + 1} dz \quad (2)$$

Strain is a measure of soil volume change ($\epsilon > 0$ for expansion or $\epsilon < 0$ collapse) and is calculated as $\epsilon(z) + 1 = (C_{i,w}(z) \cdot \rho_w(z)) / (C_{i,p} \cdot \rho_p)$ (17).

For the ridge cores sampled at SSHO, the average core $m_{Mn,w}$ is equal to $47.2 \text{ mg Mn cm}^{-2}$, indicating net enrichment of Mn in the soil relative to the parent shale. Only one core was slightly depleted in Mn (Table S1, Site N; $m_{Mn,w} = -1.8 \text{ mg cm}^{-2}$). Since erosion and chemical weathering remove Mn from the soil, external inputs must equal or exceed these outputs to result in positive values of $m_{Mn,w}$ for 20 of 21 cores.

The ratio of average $m_{Mn,w}$ to $M_{Mn,w}$ ($= 47.2/89.2 = 0.53$) is consistent with the conclusion that at least half of the Mn in ridge soils is derived from external Mn additions.

Mass Balance Model. To estimate rates of atmospheric Mn addition to SSHO, we model inputs and outputs to each sampled ridge soil using the chemical data reported here. In this model, Mn enrichment in soils changes over time as a function of varying atmospheric input rates, A ($\mu\text{g cm}^{-2} \text{ y}^{-1}$), representing dust or solutes of either natural or anthropogenic origin. Regardless of whether the excess Mn is due to natural or anthropogenic influxes, the soil thickness of each profile is presumed to be constant with time, i.e., at steady state. If the rates of erosion differed significantly from the soil production rate, ω (m My^{-1}), the soil would eventually disappear or thicken over geological timeframes (36). Ma et al. (2010) have estimated the soil production rate ω for the ridge top soils in the SSHO to equal 45 m My^{-1} based on U series isotopes (26). This soil production rate is consistent with a residence time of $\sim 7100 \text{ y}$ ($= 0.32 \text{ m}/45 \text{ m My}^{-1}$) for particles in the observed average soil thickness, L ($= 0.32 \text{ m}$), at SSHO ridges.

For our model calculations, the time zero point is a hypothetical steady state where the mass of Mn present in the ridge soil is identical to that derived from its protolith (i.e., $\tau_{Zr,Mn} = 0$; $C_{Mn,w} = 997 \mu\text{g g}^{-1}$) and is based on the assumption of no significant net additions or removals of Mn during pedogenesis. The assumption that $m_{Mn,w} = 0$ at time zero is conservative in that soils in temperate climates typically experience depletion of mobile elements, characterized by $\tau_{Zr,Mn} < 0$ (22). Thus, our estimates for the atmospheric deposition rates (A) required to explain SSHO observations will constitute a lower limit.

Under the assumption of steady state, the input and output fluxes of Mn to the soil can be calculated. At the ridge, one Mn input to the soil column is soil production (B)

$$B = C_{Mn,p} \rho_p \omega \quad (3)$$

This rate of Mn input to the soil due to soil production from bedrock, B , is assumed constant for all profiles and is calculated to equal $8.7 \mu\text{g cm}^{-2} \text{ y}^{-1}$ from the average values of the three terms in (3) reported earlier.

One outflux of Mn from ridgetop soil is physical erosion (E)

$$E = C_{Mn,w} \rho_w \omega \quad (4)$$

The loss of Mn due to physical erosion at time zero, E ($= 5.9 \pm 0.8 \mu\text{g cm}^{-2} \text{ y}^{-1}$), is calculated as the background soil Mn concentration ($C_{Mn,w} = 997 \mu\text{g g}^{-1}$ when $\tau_{Zr,Mn} = 0$) multiplied by depth-averaged soil bulk density (ρ_w) and denudation rate. For this calculation, we assume uniform Mn concentration with depth in the soil profile consistent with neither loss nor gain of Mn from the hypothetical starting point soil. With this assumption, E varies for each ridge top profile only due to different total depths that create differences in depth-averaged bulk density for each profile.

Assuming that the values for A due to atmospheric inputs are initially negligible, as dictated current observations of natural dust (Table S4), the output solute flux due to chemical weathering, W ($= 2.8 \pm 0.8 \mu\text{g cm}^{-2} \text{ y}^{-1}$), must be equal to the difference between B and E under the condition of steady state Mn mass. This value for W is compared to the modern chemical weathering flux, calculated as the difference in the Mn concentrations between influent precipitation ($C_{Mn,ppt} = 0.0025 \mu\text{g mL}^{-1}$) and effluent pore fluid ($C_{Mn,pf} = 0.082 \mu\text{g mL}^{-1}$)

$$W = MAP \left(\frac{C_{Cl,ppt}}{C_{Cl,pf}} C_{Mn,pf} - C_{Mn,ppt} \right) \quad (5)$$

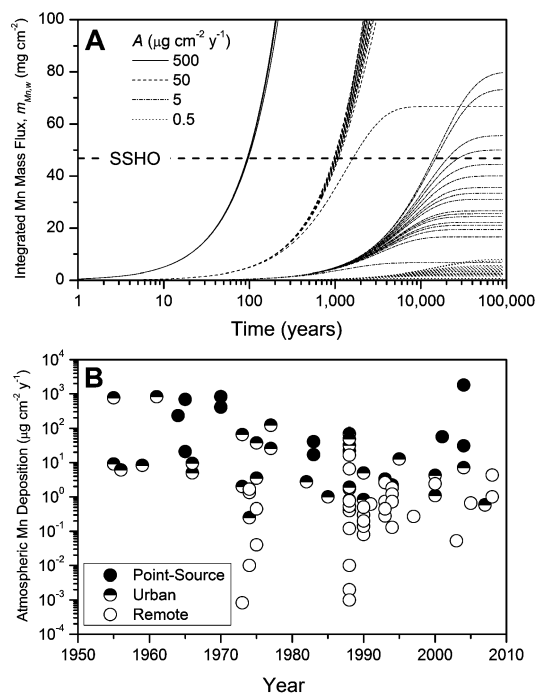


FIGURE 2. A) Model outputs for the integrated mass flux of Mn ($m_{Mn,w}$; eq 2) calculated for 21 SSHO ridge soils as a function of varying atmospheric deposition rates of Mn, A , over time. Each soil profile begins at a steady state mass of Mn consistent with $m_{Mn,w} = 0$ and is perturbed by atmospheric input of either anthropogenic ($A = 5\text{--}500 \mu\text{g cm}^{-2} \text{y}^{-1}$) or natural ($A < 5 \mu\text{g cm}^{-2} \text{y}^{-1}$) dust and solute Mn inputs at $t > 0$. The dashed horizontal line indicates the average $m_{Mn,w}$ of SSHO soils ($\sim 47 \text{ mg cm}^{-2}$). B) Rates of Mn deposition reported in the literature show decreasing deposition levels between 1950–2010, with the highest levels associated with industrial point-sources and urban areas and the lowest values associated with sites impacted only by natural processes (Table S4).

These concentrations are corrected for evapotranspiration using the standard correction based on Cl concentrations in pore fluid ($C_{Cl,pf} = 1.3 \mu\text{g mL}^{-1}$) and influent precipitation (30) ($C_{Cl,ppi} = 0.20 \mu\text{g mL}^{-1}$), with mean annual precipitation, $MAP = 104.9 \text{ g cm}^{-2} \text{y}^{-1}$. The modern value for W ($= 1.0 \mu\text{g cm}^{-2} \text{y}^{-1}$) is slightly less than the calculated initial steady state estimate; therefore, the steady state values for W ($= 2.8 \pm 0.8 \mu\text{g cm}^{-2} \text{y}^{-1}$) will be used in the model as an upper limit estimate of chemical weathering.

In the model calculation after time zero, Mn is input to the soil through atmospheric deposition, A , perturbing the soil profile away from steady state with respect to Mn mass. B and W are held constant, but E is allowed to change over time as the Mn concentrations in the soil profile change with time (see eq 4). In Figure 2a, we show values of $m_{Mn,w}$ for SSHO soils calculated over time for different values of A representing short-term “anthropogenic” and long-term “natural mineral dust” fluxes. The values for anthropogenic ($5\text{--}500 \mu\text{g cm}^{-2} \text{y}^{-1}$) and natural ($0.5\text{--}5 \mu\text{g cm}^{-2} \text{y}^{-1}$) Mn deposition are order of magnitude estimates representing measurements compiled from the literature (Figure 2b; Table S4). Soil profiles receiving Mn as natural mineral dust or solutes ($A = 0.5 \mu\text{g cm}^{-2} \text{y}^{-1}$) reach a new steady state level for $m_{Mn,w}$ well below the average calculated value for SSHO soil profile data. Only 4 out of 21 soil profiles reach SSHO enrichment of Mn with inputs of $A = 5 \mu\text{g cm}^{-2} \text{y}^{-1}$, the upper level “natural” and lower level “anthropogenic” rate, and even this does not occur within the soil residence time ($< 7100 \text{ y}$). Therefore, inputs of mineral dust, even over time scales much longer than the residence time of the soils, are generally insufficient to explain the Mn enrichment. In

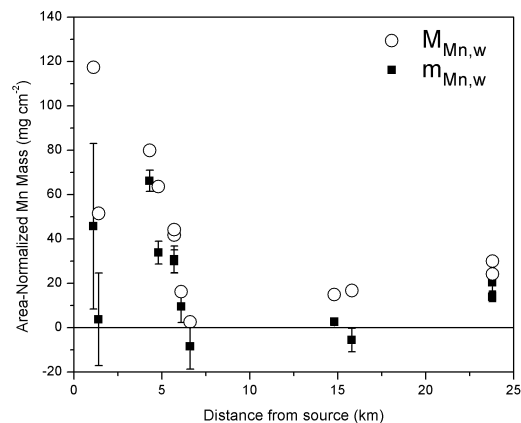


FIGURE 3. The total area-normalized Mn mass ($M_{Mn,w}$; \circ) and integrated mass flux of Mn ($m_{Mn,w}$; \blacksquare) are shown for 12 soil cores augered at distances between 1 to 24 km from the steel plant source at Burnham, PA. Soils near the plant are elevated in Mn relative to soils further away. Error bars for $m_{Mn,w}$ represent the standard deviations in calculated mass flux values for each core as described in the text. Error bars for $M_{Mn,w}$ represent analytical error in $C_{Mn,w}$ ($\pm 3\%$) and are smaller than symbols. Large standard deviations result mostly from variability in measured compositions of samples used to infer parent composition.

contrast, the Mn concentrations observed in the soils are consistent with anthropogenic levels of A over industrial time scales. For example, at $A = 500 \mu\text{g cm}^{-2} \text{y}^{-1}$, $m_{Mn,w}$ reaches the SSHO average value of 47.1 mg cm^{-2} within 100 years. Mn enrichment in SSHO soils is therefore best explained as the result of industrial deposition.

Burnham Soils. To understand the implications of this interpretation, we investigated soils around the Standard Steel, LLC steel manufacturing plant located $\sim 28 \text{ km}$ southeast of SSHO in Burnham, PA. Within $\sim 6 \text{ km}$ of the facility, Mn concentrations are high in surface soils ($1600 \pm 700 \mu\text{g g}^{-1}$) relative to deep soils ($300 \pm 100 \mu\text{g g}^{-1}$) with $m_{Mn,w}$ values ($\sim 35 \text{ mg cm}^{-2}$) comparable to SSHO (Figure 3; Figure S2; Table S2). In contrast, soils sampled far from roads at points 15–16 km away from the plant contain relatively low Mn ($200 \pm 100 \mu\text{g g}^{-1}$) at all depths and $m_{Mn,w} < 10 \text{ mg cm}^{-2}$. Soils collected $\sim 24 \text{ km}$ away and within 50 m of a state road have slightly elevated Mn concentrations and $m_{Mn,w} \approx 17 \text{ mg cm}^{-2}$, consistent with contamination due to vehicular exhaust (3, 9).

For the Burnham sites, we compare values for $\tau_{Ti,Mn}$ and $m_{Mn,w}$ using two different assumptions for parent: 1) parent composition assumed equal to the deepest augered sample from each core and 2) parent composition equal to the average composition of all the deepest augered samples from all cores. Ti was used as the immobile element and strain values were calculated using SSHO bulk density measurements. Although the total mass of soil Mn ($M_{Mn,w}$) is highest near the source, estimates of $m_{Mn,w}$ have large standard deviations due to variability in inferred parent compositions. Even with these considerations, soils nearest to Burnham are enriched in Mn relative to those further away.

Soil Chemistry Compilations. To assess whether the inferred Mn contamination in these central Pennsylvania soils was unusual, we collated available geochemical data for United States and European soils. For the U.S., we combined 385 chemical profiles for U.S. soils from the Natural Resources Conservation Service’s Spatial Geochemical Database ($n = 290$) with as many published studies as we were able to find with the requisite data ($n = 95$) (36–41). For the U.S. soils, we used every data set we found that provided i) chemical composition of C horizon soil or parent, ii) concentrations for at least 3 depth intervals covering 2/3 of

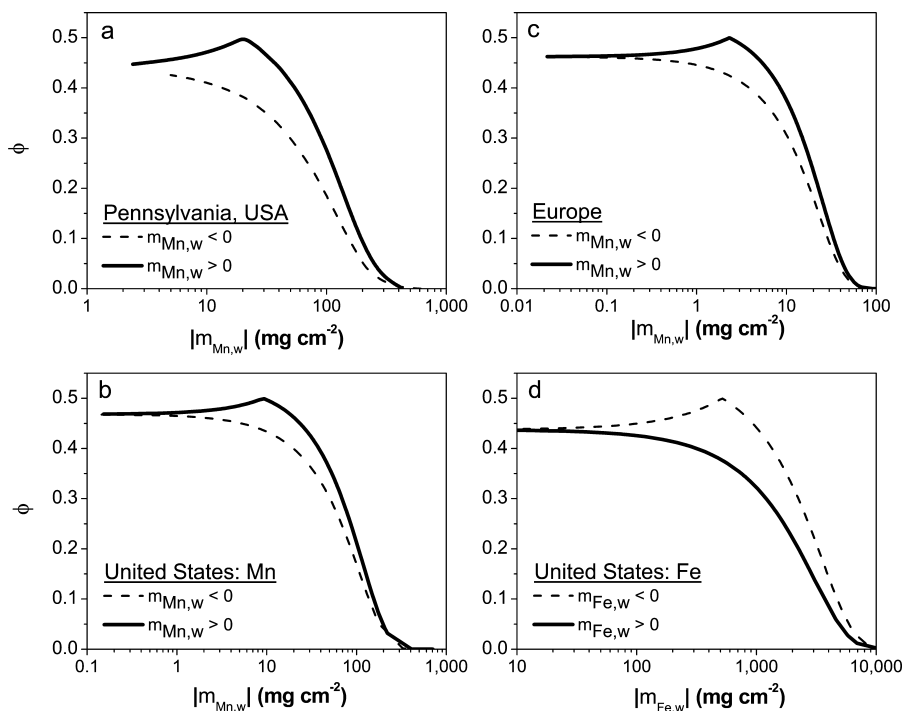


FIGURE 4. Distributions of calculated $m_{Mn,w}$ (eq 2) for reported soil chemistry in Pennsylvania (a), the United States (b), and Europe (c) and $m_{Fe,w}$ for soils in the United States (d) (see text for data set attributions). Values of $m_{Mn,w}$ for each data set were fit to a normal distribution to determine the fraction (ϕ) of measurements falling above or below values of $m_{Mn,w}$. Values of ϕ are plotted for the absolute values of $m_{j,w}$, where net enrichment ($m_{j,w} > 0$) is plotted as a solid line and net depletion ($m_{j,w} < 0$) as a dashed line. The mean of each data set (the value at the peak where $\phi = 0.5$) documents that net enrichment of Mn is more common than depletion in soils in Pennsylvania, the United States, and Europe, but depletion is more common for Fe in the United States.

total pedon depth to parent, and iii) concentrations of both Mn and an insoluble element. For the European soils, enrichment of Mn in topsoil (0–25 cm depth) was calculated relative to the C horizon from data reported in the Geochemical Baseline Mapping Programme (42). The FOREGS database has been previously used to predict heavy metal distribution in topsoils based on various factors (e.g., parent lithology, topography, population density) (43), and MnO distribution had been found to potentially correlate with anthropogenic influence (44). Similar to the approach we used in the Burnham calculations, total Mn influx or outflux to each pedon ($m_{Mn,w}$; eq 2) was evaluated using Ti as the immobile element since Ti concentrations were reported more often than Zr and Ti is relatively immobile in many soils (17, 45). Since no bulk density data were available for bedrock or soils in the compilations, parent bulk density was set equal to that of the Rose Hill Shale (2.4 g cm^{-3}), and soils were assumed to weather isovolumetrically ($\epsilon = 0$). Differences among common lithological bulk densities introduce only small variability to the calculated $m_{Mn,w}$ value.

All of these data sets define positively skewed distributions consistent with the majority of soils demonstrating Mn addition rather than depletion (Figure 4). For Pennsylvania soils ($n = 64$), $m_{Mn,w}$ averages 20 mg cm^{-2} , and $\sim 70\%$ of the soils show $m_{Mn,w} > 0$. For the U.S. data set ($n = 385$), $m_{Mn,w}$ averages 16 mg cm^{-2} with $>60\%$ of profiles showing Mn enrichment. A map of $m_{Mn,w}$ in the United States reveals the sparseness of the available soils data for trace metals (Figure S3). In Europe, the mean topsoil Mn concentrations ($620 \pm 510 \mu\text{g g}^{-1}$) are only slightly higher than C horizon concentrations ($570 \pm 460 \mu\text{g g}^{-1}$), and average values of $m_{Mn,w} = 2.4 \text{ mg cm}^{-2}$ document that 51% of the soils show enrichment. However, a map of the data shows large spatial variance and a concentration of enriched sites near industrialized regions (Figure S4). The data therefore document that the spatial heterogeneity in values of $m_{Mn,w}$ is large but that a significant

number of soils sampled in PA, the U.S., and Europe are consistent with Mn contamination.

Patchiness of the Mn contamination in soils is attributed partly to the existence of point sources of Mn emission to the atmosphere, including steel plants and coal-burning power plants, as well as more diffuse contributions from gasoline (3, 5, 9, 11). However, widespread dissemination of anthropogenic Mn to the atmosphere has been documented as deposition to the ocean over thousands of kilometers in the North Atlantic (13). The patchiness of soil Mn is therefore presumably not just due to the localized nature of the source but is also due to the variability of soils themselves. For example, in the Pennsylvania data set, Mn is enriched in soils developed on basic crystalline rock, limestone, and shale, while soils derived from sandstones exhibit net Mn depletion (36–38). Thus, patchiness in the soil Mn enrichment may also be related to patchiness of lithologies that outcrop at Earth's surface. Finally, vegetation acts as a capacitor in that it biolifts, stores, and recycles the Mn (34), and different vegetation types presumably cause or exacerbate the patchiness.

The evidence for common but spatially heterogeneous Mn contamination in industrialized areas is amplified by observations of Pb and Cd concentrations, two other trace metals that are known to be heavily impacted by human activity (11, 46). The data from the European topsoils also show positively skewed distributions for Pb and Cd similar to Mn (Figure S5). In contrast, the distribution of $m_{Fe,w}$ in U.S. soils is negatively skewed toward Fe depletion (Figure 4d) even though Mn and Fe are leached from soils at comparable redox conditions (28). Mn enrichment concurrent with Fe depletion is consistent with Mn additions. In these soils, Fe fluxes have been dominated by depletion, while Mn fluxes have been dominated by atmospheric inputs.

Additional research is needed to assess the global impacts of atmospheric deposition on soil geochemistry and ecological processes. Numerous trace metals are discharged to the air by anthropogenic activities, yet there remains a distinct lack of knowledge on where these elements are deposited, in which environmental pools they accumulate, and the rates of transfer among these pools. The increased availability of global soil data through compilation efforts would facilitate the documentation of long-term anthropogenic metal inputs to ecosystems worldwide.

Acknowledgments

This material is based upon work supported by the National Science Foundation under Grant No. CHE-0431328 for the Center for Environmental Kinetics Analysis and under Grant No. EAR-0725019 to Chris Duffy (Penn State) for the Susquehanna Shale Hills Critical Zone Observatory. The authors would like to acknowledge Danielle Andrews, Jennifer Williams, and other members of the Susquehanna Shale Hill Observatory for help with soil and water sample collection.

Supporting Information Available

Additional figures and tables presenting data discussed in the main article. This material is available free of charge via the Internet at <http://pubs.acs.org>.

Literature Cited

- (1) Post, J. E. Manganese oxide minerals: Crystal structures and economic and environmental significance. *Proc. Natl. Acad. Sci.* **1999**, *96*, 3447–3454.
- (2) Manceau, A.; Gorshkov, A. I.; Drits, V. A. Structural chemistry of Mn, Fe, Co, and Ni in manganese hydrous oxides: Part II. Information from EXAFS spectroscopy and electron and X-ray diffraction. *Am. Mineral.* **1992**, *77*, 1144–1157.
- (3) U.S. Environmental Protection Agency. *Health Assessment Document for Manganese: Final Report*; Report No. EPA-600/8-83-013F; Cincinnati, OH, 1984.
- (4) Garrels, R. M.; Mackenzie, F. T.; Hunt, C. *Chemical cycles and the global environment - assessing human influences*; W. Kaufman, Inc.: Los Altos, CA, 1975.
- (5) *National Academy of Sciences. Manganese: Medical and Biologic Effects of Environmental Pollutants*; National Academy Press: Washington, DC, 1973.
- (6) Rahn, K. A.; Lowenthal, D. H. Pollution aerosol in the northeast: northeastern-midwestern contributions. *Science* **1985**, *228*, 275–284.
- (7) Nriagu, J. O.; Pacyna, J. M. Quantitative assessment of worldwide contamination of air, water and soils by trace metals. *Nature* **1988**, *333*, 134–139.
- (8) Parekh, P. P. A study of manganese from anthropogenic emissions at a rural site in the eastern United States. *Atmos. Environ.* **1990**, *24A*, 415–421.
- (9) Lytle, C. M.; Smith, B. N.; McKinnon, C. Z. Manganese accumulation along Utah roadways: a possible indication of motor vehicle exhaust pollution. *Sci. Total Environ.* **1995**, *162*, 105–109.
- (10) Brewer, R.; Belzer, W. Assessment of metal concentrations in atmospheric particles from Burnaby Lake, British Columbia, Canada. *Atmos. Environ.* **2001**, *35*, 5223–5233.
- (11) Pacyna, J. M.; Pacyna, E. G. An assessment of global and regional emissions of trace metals to the atmosphere from anthropogenic sources worldwide. *Environ. Rev.* **2001**, *9*, 269–298.
- (12) Boudissa, S. M.; Lambert, J.; Muller, C.; Kennedy, G.; Gareau, L.; Zayed, J. Manganese concentrations in the soil and air in the vicinity of a closed manganese alloy production plant. *Sci. Total Environ.* **2006**, *361*, 67–72.
- (13) Buck, C. S.; Landing, W. M.; Resing, J. A.; Measures, C. I. The solubility and deposition of aerosol Fe and other trace elements in the North Atlantic Ocean: Observations from the A16N CLIVAR/CO2 repeat hydrography section. *Mar. Chem.* **2008** doi: 10.1016/j.marchem.2008.08.003.
- (14) Suarez, D. L.; Langmuir, D. Heavy metal relationships in a Pennsylvania soil. *Geochim. Cosmochim. Acta* **1976**, *40*, 589–598.

- (15) Kogelmann, W. J.; Sharpe, W. E. Soil acidity and manganese in declining and nondeclining sugar maple stands in Pennsylvania. *J. Environ. Qual.* **2006**, *35*, 433–441.
- (16) Horsley, S. B.; Long, R. P.; Bailey, S. W.; Hallett, R. A.; Hall, T. J. Factors associated with the decline disease of sugar maple on the Allegheny Plateau. *Can. J. For. Res.* **2000**, *30*, 1365–1378.
- (17) Brimhall, G. H.; Dietrich, W. E. Constitutive mass balance relations between chemical composition, volume, density, porosity, and strain in metasomatic hydrochemical systems: Results on weathering and pedogenesis. *Geochim. Cosmochim. Acta* **1987**, *51*, 567–587.
- (18) Chadwick, O. A.; Brimhall, G. H.; Hendricks, D. M. From a black box to a gray box - a mass balance interpretation of pedogenesis. *Geomorphology* **1990**, *3*, 369–390.
- (19) Chadwick, O. A.; Derry, L. A.; Vitousek, P. M.; Huebert, B. J.; Hedin, L. O. Changing sources of nutrients during four million years of ecosystem development. *Nature* **1999**, *397*, 491–497.
- (20) Kurtz, A. C.; Derry, L. A.; Chadwick, O. A. Accretion of Asian dust to Hawaiian soils: Isotopic, elemental, and mineral mass balance. *Geochim. Cosmochim. Acta* **2001**, *65*, 1971–1983.
- (21) Porder, S.; Hilley, G. E.; Chadwick, O. A. Chemical weathering, mass loss, and dust inputs across a climate by time matrix in the Hawaiian islands. *Earth Planet. Sci. Lett.* *258*, 414–427.
- (22) Brantley, S. L.; White, A. F. Approaches to modeling weathered regolith. In *Thermodynamics and Kinetics of Water-Rock Interaction*; Oelkers, E. H., Schott, J. Eds.; The Mineralogical Society of America: Chantilly, VA, 2009; Vol. 70, pp 435–484.
- (23) Lin, H.; Kogelmann, W.; Walker, C.; Bruns, M. A. Soil moisture patterns in a forested catchment: A hydrogeological perspective. *Geoderma* **2005**, *131*, 345–368.
- (24) Lin, H. Temporal stability of soil moisture spatial pattern and subsurface preferential flow pathways in the Shale Hills catchment. *Vadose Zone J.* **2006**, *5*, 317–340.
- (25) Jin, L.; Ravella, R.; Ketchum, B.; Heaney, P.; Brantley, S. L. Mineral weathering and element transport during hillslope evolution at the Susquehanna/Shale Hills Critical Zone Observatory. *Geochim. Cosmochim. Acta* **2010**, *74*, 3669–3691.
- (26) Ma, L.; Chabaux, F.; Pelt, E.; Blaes, E.; Jin, L.; Brantley, S. Regolith production rates calculated with Uranium-series isotopes at Susquehanna Shale Hills Critical Zone Observatory. *Earth Planet. Sci. Lett.*, accepted.
- (27) National Academy of Sciences. *Basic Research Opportunities in Earth Science*; NRC; National Academy Press: Washington, DC, 2001.
- (28) Schatzel, R.; Anderson, S. *Soils genesis and geomorphology*; University Press: Cambridge, U.K., 2002.
- (29) Stine, H. E. *The Story of Juniata Iron*. Master's Thesis. The American University, Washington, DC, 1964.
- (30) National Atmospheric Deposition Program. <http://nadp.sws.uiuc.edu/> (accessed month day, year).
- (31) Hoskins, D. M. Burnham Quadrangle. In *Atlas of Preliminary Geologic Quadrangle Maps of Pennsylvania*; PA Geological Survey, 1981.
- (32) *Bedrock geologic map of the Allensville Quadrangle, Huntingdon and Mifflin Counties Pennsylvania*; Pennsylvania Geological Survey; OFBM 07-02.0, 2007.
- (33) Anderson, S. P.; Dietrich, W. E.; Brimhall, G. H. Weathering profiles, mass-balance analysis, and rates of solute loss: Linkages between weathering and erosion in a small, steep catchment. *GSA Bull.* **2002**, *114*, 1143–1158.
- (34) Jobbagy, E. G.; Jackson, R. B. The uplift of soil nutrients by plants: biogeochemical consequences across scales. *Ecology* **2004**, *85*, 2380–2389.
- (35) Egli, M.; Fitze, P. Formulation of pedogenic mass balance based on immobile elements: a revision. *Soil Sci.* **2000**, *165*, 437–443.
- (36) Ciolkosz, E. J.; Rose, A. W.; Waltman, W. J.; Thurman, N. C. Total elemental analysis of Pennsylvania soils. The Pennsylvania State University Agronomy Series 1993; No. 126.
- (37) Ciolkosz, E. J.; Amistadi, M. K.; Thurman, N. C. Metals in Pennsylvania soils. The Pennsylvania State University Agronomy Series 1993; No. 128.
- (38) Ciolkosz, E. J. Major and trace elements in southwestern Pennsylvania soils. The Pennsylvania State University Agronomy Series 2000; No. 148.
- (39) Teusch, N.; Erel, Y.; Halicz, L.; Chadwick, O. A. The influence of rainfall on metal concentration and behavior in the soil. *Geochim. Cosmochim. Acta* **1999**, *63*, 3499–3511.
- (40) Muhs, D. R.; Bettis, E. A.; Been, J.; McGeehin, J. P. Impact of climate and parent material on chemical weathering in loess-derived soils of the Mississippi River Valley. *Soil Sci. Soc. Am. J.* **2001**, *65*, 1761–1777.

- (41) National Cooperative Soil Characterization Data. <http://soils.usda.gov/survey/geochemistry/> (accessed October 9, 2008).
- (42) Geochemical Atlas of Europe. <http://www.gtk.fi/publ/foregsatlas/> (accessed December 23, 2008).
- (43) Lador, L. R.; Hengl, T.; Reuter, H. Heavy metals in European soils: A geostatistical analysis of the FOREGS Geochemical database. *Geoderma* **2008**, *148*, 189–199.
- (44) Imrie, C. E.; et al. Application of factorial kriging analysis to the FOREGS European topsoil geochemistry database. *Sci. Total Environ.* **2008**, *393*, 96–110.
- (45) Neaman, A.; Chorover, J.; Brantley, S. L. Effects of organic ligands on granite dissolution in batch experiments at pH 6. *Am. J. Sci.* **2006**, *306*, 451–473.
- (46) Rauch, J. N.; Pacyna, J. M. Earth's global Ag, Al, Cr, Cu, Fe, Ni, Pb and Zn cycles. *Global Biogeochem. Cycles* **2009**, *23*, GB2001, doi:10.1029/2008GB003376.

ES102001W